JOURNAL OF KUFA–PHYSICS
www.uokufa.edu.iq/journals/index.php/jkp | ISSN: 2077–5830

# A Theoretical Study of $H_2S$ Toxic Gas Adsorption on Pristine and Doped Monolayer $(AlN)_{21}$ Using Density Functional Theory

***Jamal A. Shlaka** **Abbas H. Abo Nasria**

*Department of Physics, Faculty of Science, University of Kufa, Najaf, Iraq.*

*Corresponding Author E-mail: jamala.alabbasy@student.uokufa.edu.iq

**ARTICLE INF**

***Article history:***
Received: 17 JUL, 2020
Revised: 12 SEP, 2020
Accepted: 20 SEP, 2020
Available Online: 31 DEC, 2020

***Keywords:***

Graphene, (DFT) method
Physisorption
Sensors
Chemisorption

**ABSTRACT**

Been studying the interactions between graphene - like aluminium nitride **P**$(AlN)_{21}$ nano ribbons doped and defect $(AlN)_{21}$Sheet, Molecules and small toxic gas molecules ( $H_2S$), were built for two different adsorption sites on graphene like aluminium nitride **P**$(AlN)_{21}$. this was done by employing B3LYP density functional theory (DFT) with 6-31G*(d,p) using Gaussian 09 program, Gaussian viw5.0 package of programs and Nanotube Modeller program 2018. the adsorptions of $H_2S$ on P$(AlN)_{21}$, (C) atoms-doped P$(AL\text{-}N)_{20}$ sheet, D-P$(AL\text{-}N)_{20}$ and D-(C)atoms-doped P$(AL\text{-}N)_{19}$ (on atom) with ($E_{ad}$) (**-0.468**eV),(**-0.473** eV), (**-0.457** eV), (**-0.4478** eV) and (**-0.454** eV), respectively, ($E_{ad}$) of $H_2S$ on the center ring of the P$(AL\text{-}N)_{21}$, (C) atoms-doped P$(AL\text{-}N)_{20}$ sheet, D-P$(AL\text{-}N)_{20}$ and D-(C,B)atoms-doped P$(AL\text{-}N)_{19}$ sheet are (-**0.280** eV),(**-0.465** eV), (**-0.405** eV), (**-0.468** eV) and **-0.282** eV), respectively, are weak physisorption .

However, the adsorptions of $H_2S$, on the ($(AlN)_{20}$ -B and D-$(AlN)_{19}$ -B), (on atom N and center ring the sheet) are a strong chemisorption because of the ($E_{ad}$) larger than -0.5 eV, due to the strong interaction, the ($(AlN)_{20}$-B and D-$(AlN)_{19}$-B), could catalyst or activate, through the results that we obtained, which are the improvement of the sheet **P**$(AlN)_{21}$ by doping and per forming a defect in, it that can be used to design sensors.

DOI: http://dx.doi.org/10.31257/2018/JKP/2020/120210

## دراسة نظرية لامتزاز غاز كبريتيد الهيدروجين السام على نتريت الالمنيوم احادي الطبقة باستخدام نظرية دالية الكثافة الوظيفية

**جمال عبد زيد شلاكة** **عباس حسن ابو ناصرية**

جامعة الكوفة/كلية العلوم/قسم الفيزياء

**الكلمات المفتاحية:**

الكرافين

**الـــخُـــلاصـــة**

تـم مـن خـلال نظريـة (DFT) دراسـة التفـاعلات بـين نيتريـد الألومنيـوم شـبيه الكـرافين

كشرائح نانوية مطعمة بالكاربون والبورون ومشوهة $(AlN)_{21}$ P، {P (AlN) 21}, (PG) D-، D-P $(AlN)_{20}$، $(AlN)_{19}$-B2، $(AlN)_{20}$-B، $(AlN)_{19}$-C2، (AlN) 20-C، $(AlN)_{19}$-C، D-$(AlN)_{18}$-C2، D-$(AlN)_{19}$-B، D-$(AlN)_{18}$-B2 مع جزيئة الغاز السام الصغيرة ($H_2S$) ، حيث تم وضعها في موقعين مختلفين للتفاعل على نيتريد الألومنيوم $(AlN)_{21}$ P، وقد تم ذلك باستخدام نظرية داليـة الكثافـة (DFT) مـع B3LYP، 6-31G*(p,d) باستخدام مجموعة البرامج (Gaussian09 viw5.0 وبرنامج Nanotube Modeller 2018)، فقد تفاعل غاز $H_2S$ تفاعلا ضعيفا (physisoption) ايضا مع جميع الجزيئات الا الجزيئة المطعمة بالبورون وبدون تشويه $P(AlN)_{21}$ و$(AlN)_{20}$-C، D-P $(AlN)_{20}$، D- $(AlN)_{19}$-C ، D-$(AlN)_{19}$-B وكانت طاقات الامتزاز للجزيئات اعلاه كما يلي : (-0.468eV) و (-٠.٤٧٣ eV) و( -0.457 eV) (-٠.٤٧٨ eV) و (-٠.٤٥٤ eV) على التوالي ، اما طاقات الامتزاز عندما تكون جزيئة الغاز عموديا على مركز الحلقة فهي كما يلي (-٠.٢٨٠ eV) و (-0.465 eV)، ( -0.405 eV)، (0.468 eV) و (-٠.٢٨٢ eV) على التوالي ، وكل ما سبق من الجزيئات يعطينا مستشعرًا جيدًا لـ $H_2S$، ومن جهة اخرى فإن تفاعل $H_2S$ ، علىB-$(AlN)_{20}$ ، (علـى ذرة N ووسـط الحلقـة) هـو تفاعـل كيميـائي قـوي (chemisoption) لأن $E_{ad}$ أكبر من (-٠.٥ eV)، بسبب التفاعل القوي لذلك ممكن استخدامه كعامل محفز او مساعد في التجارب الكيميائية (catclyst).

التفاعل الفيزيائي الضعيف
المتحسسات
التفاعل الكيميائي القوي

## 1. INTRODUCTION

Graphene like-material attracted a tremendous scientific and technological attention as the new honeycomb. Its exceptional physical and chemical properties[1,2], such as high surface area, superior electrical conductivity, and huge mechanical strength[3]. It has been led to many applications in various fields of study, such as compound materials, solar-cell technology, liquid crystal devices, Catalyst, and gas adsorbent. Graphene-based nanostructures and Graphene like-material are well known to be great to improve the potential of various sensors. Normally pristine aluminium nitride $(AlN)_{21}$ sheet, graphene like-material properties is a weak adsorbent/sensor device because it has two-dimensional (2D) structure[4,5] with the surface only and no volume, which exploits the interaction of surface dopants with adsorbents. Therefor to increase its sensitivity[6,7], by deliberately doped pristine $(AlN)_{21}$ sheet with B and C elements and deformation. It should be noticed that because of 2D structure of pristine $(AlN)_{21}$ sheet[4], there is a space limitation for nearing the large molecules on its surface. As a result, it may not be the best choice to use pristine $(AlN)_{21}$ sheet for adsorption process of large molecules. To solving this problem, B and other elements-doped $(AlN)_{21}$ sheet will be an ideal choice because of significant changing in the structure of$(AlN)_{21}$ sheet. It has been recognized that C doping could attain the highest sensitivity of $(AlN)_{21}$ sheet toward different chemicals, and the applications of $(AlN)_{21}$ sheet could be mainly enhanced. Graphene and its relatives belong to the new active research area towards adsorption of gas molecules. It has been verified that the reinforcement in the charge concentration of $(AlN)_{21}$ sheet after adsorption of gas molecule can be used to create highly sensitive sensors. The modificationin the resistivity due to gas adsorbed on $(AlN)_{21}$(including pristine, B or C doped and defective aluminium nitride sheet) sheet corresponds to sensing properties that may

be considered as acceptors or donors. In addition, special binding sites in $(AlN)_{21}$sheet can help to understand of interactions near the surface. Several theoretical researches based on density functional theory (DFT) calculations have been done to demonstrate the energies of interaction between small molecules with a $(AlN)_{21}$sheet [8,9]. Theoretical studies indicate that the replacement of atom by doping or deforming can alter the band structure of $(AlN)_{21}$ sheet and thus, the applications of $(AlN)_{21}$ sheet could be mainly enhanced and expanded. Based on the kind of dopant, there are many papers showing the enhanced properties of graphene[10,11] among them, B and C are of the most used dopants toward doping process for different purpose [12].

In the present work, DFT calculations were performed to simulate the adsorption of and ($H_2S$) gas molecule on the surface of $(AlN)_{21}$ sheet as well as (B and C)-doped$(AlN)_{21}$sheet and to investigate their effect on the electronic properties of these surfaces. It is doubted that the incorporation company alters the structure of graphene and raised its quality.

## 2. Computational Details Of DFT

In this work, All calculations were carried out using DFT[13], the geometric structures were completely optimized using Gaussian 09 program package with Gauss View 5.0.8 program. The Perdew, Burke, and Ernzerhof (PBE) exchange-correlation functional were chosen [14], to describe the exchange and correlation energy in the structural optimizations and total energy calculations. The system is modeled including 21 (Al and N) atoms of Pristine as well as (C and B) -doped (Al-N) sheet and deformation was created.. The $E_{ad}$ of molecules on the P(Al-N) sheet ($E_{ad\ (gas+\ P(Al-N)\ sheet)}$) and (C or B)-doped (Al-N) sheet $E_{ad\ (gas+(\ C\ or\ B)\text{-doped P(Al-N) sheet})}$ is defined as follows:

$$E_{ad\ (gas+\ P\ (Al\text{-}N)\ sheet)} = E_{(gas+\ P(Al\text{-}N)\ sheet)} - (E_{\ P(Al\text{-}N)\ sheet} + E_{gas}) \quad (1)$$

$$E_{ad\ (gas+\ (C\ or\ B)\text{-doped P(Al-N) sheet})} = E_{(gas+\ (C\ or\ B)\text{-doped P(Al-N) sheet})} - (E_{(C\ or\ B)\text{-doped P(Al-N) sheet}} + E_{gas}) \quad (2)$$

where $E_{(gas+P(Al\text{-}N)\ sheet)}$ and $E_{(gas+(C\ or\ B)\text{-doped P(Al-N) sheet})}$ are the total energies of the relaxed molecule on the P(AL-N) sheet and (C or B)-doped P(AL-N) sheet[8,9], respectively, $E_{P(Al\text{-}N)\ sheet}$ and $E_{(C\ or\ B)\text{-doped P(Al-N) sheet}}$ are the energies of the isolated P(AL-N) sheet and (C or B)-doped P(AL-N) sheet and $E_{gas}$ is the energy of isolated gas molecule. The diversity of relative energy of the highest occupied molecular orbital (HOMO) and the lowest unoccupied molecular orbital (LUMO) of free (C or B)-doped P(AL-N) sheet and adsorbed molecule on (C or B)-doped P(AL-N) sheet gives the mechanism of interaction. The HOMO can be defined as an electron donor because of having the excess of electrons whereas the LUMO is lacking electrons and therefore it has a power of accepting electrons[10,11].

## 3. Result and discussion

Electronic Properties of Adsorbed $H_2S$ Molecule on $P(AlN)_{21}$, (C, B)-doped $P(AlN)_{20}$ , D-$P(AlN)_{20}$ and D-(C, B)-doped $P(AlN)_{19}$

The AlN sheet has a typical graphene-like structure. The lengths of bands of the Al-N, Al- C and Al-B are 1.868 Å,1.936 Å and 2.025 Å, respectively, which are consistent with the findings in recent studies [15]. Our discussion begins with adsorption $H_2S$ gas molecule, on the $P(AlN)_{21}$ sheet. As shown in Fig.(1), there are two different adsorption sites,(on the atom and the hollow center ring) which are the hollow center of the Al-N hexagon (a), the hollow center ring of Al-N (b), the top of the C atoms (c) , the top of the hollow center ring of( Al-C) atoms (d), the top of the B

atoms (e) the hollow center ring of Al-B (f), the top of the N atoms with defect $P(AlN)_{20}$sheet (g) , the hollow center ring of defect $P(AlN)_{20}$ sheet (h) , the top of the N atoms with defect $P(AlN)_{19}$ –C sheet (i) , the hollow center ring of defect $P(AlN)_{19}$ –C sheet (j) , the top of the N atoms with defect $P(AlN)_{19}$ –B sheet (k) , the hollow center ring of defect $P(AlN)_{19}$ –B sheet (l) . The gas molecule is initially placed with its the top of the atoms center of mass exactly located at these sites. For each site,the configurations with gas were then examined. Gas molecule is initially placed vertically to the surface of AlN sheet for all the possible adsorption sites. For the gas molecule/AlN systems, the adsorption energy is defined as.

$$E_{ad} = E_{gas} + E_{AlN} - E_{gas/AlN} \quad (3)$$

$$E_f = 1/2(HOMO+LUMO) \quad (4)$$

which basically decreases and increases corresponding to the electrons decrease and increase in the elements . From fig.(1) (a) the side view of gas molecules $H_2S$ adsorb on atom of $P(AlN)_{21}$ on the distance (2.66 Å), the fig (b) shows that the gas $H_2S$ on the center ring of $P(AlN)_{21}$ with (2.64 Å) the gas $H_2S$ of the doped atom (C- doped $P(AlN)_{20}$) on the distance (2.85 Å) it note that on the fig c , fig(d) gas molecular on the center ring C- doped $P(AlN)_{20}$. on the distance (2.57 Å), the gas $H_2S$ of the doped atom (B- doped $P(AlN)_{20}$) on the distance (1.91 Å) is observed that on the fig e , fig(f) gas molecular on the center ring B- doped $P(AlN)_{20}$, for the distance (2.63 Aº), the gas $H_2S$ of the N atom in the D-$P(AlN)_{20}$ sheet for the distance (2.91Aº) we see that on the fig (g) , fig(h) gas molecular on the center ring the D-$P(AlN)_{20}$ sheet, on the distance(2.55Aº), the gas $H_2S$ of the C atom in D-$(AlN)_{19}$ –C sheet on the fig(i) on the distance(2.39Aº), gas molecular on the center ring the D-$(AlN)_{19}$ –C sheet, on the distance(2.61Aº), we see that on the fig (j), the gas $H_2S$ of the B atom in D-$(AlN)_{19}$ –B sheet on the fig(k) on the distance(2.21Aº), ), gas molecular on the center ring the D-$(AlN)_{19}$ –B sheet, on the distance(2.65Aº), we see that on the fig (l).

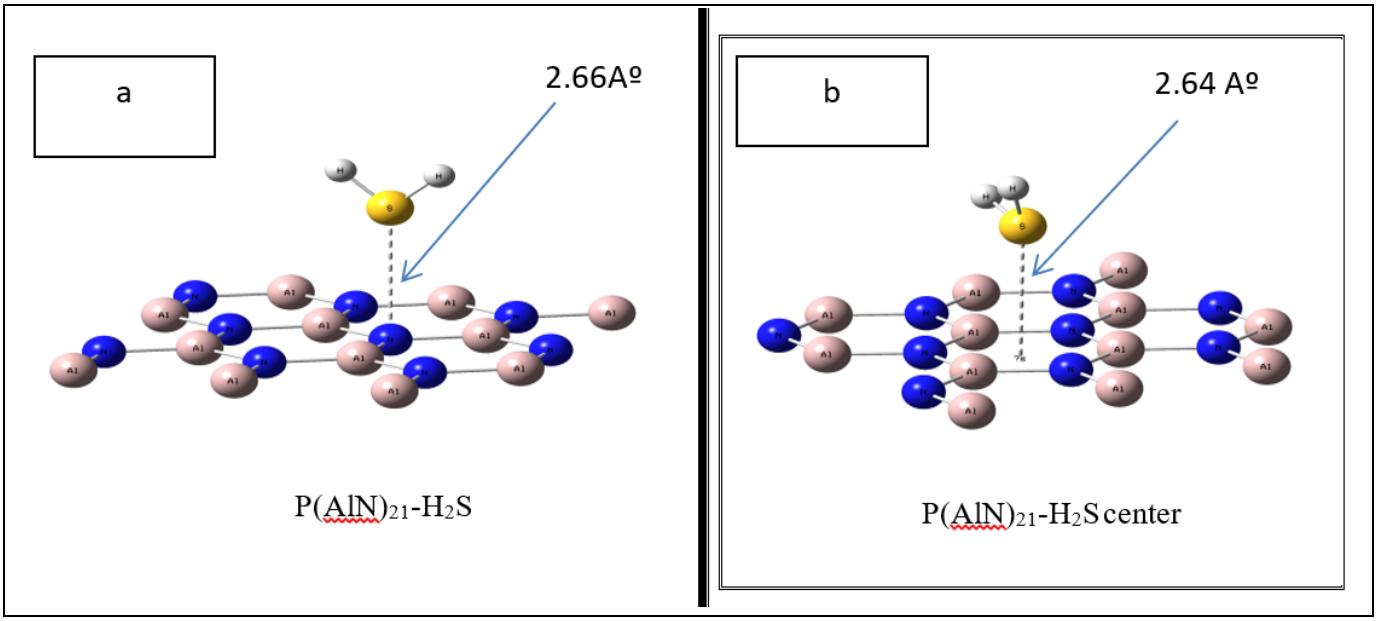

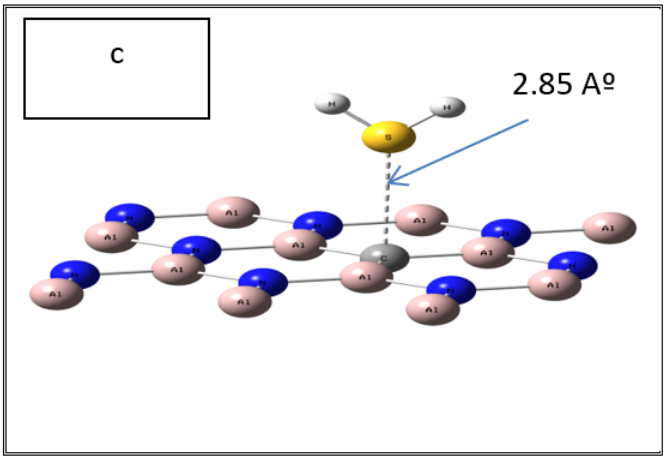


$(AlN)_{20}$–C-$H_2S$

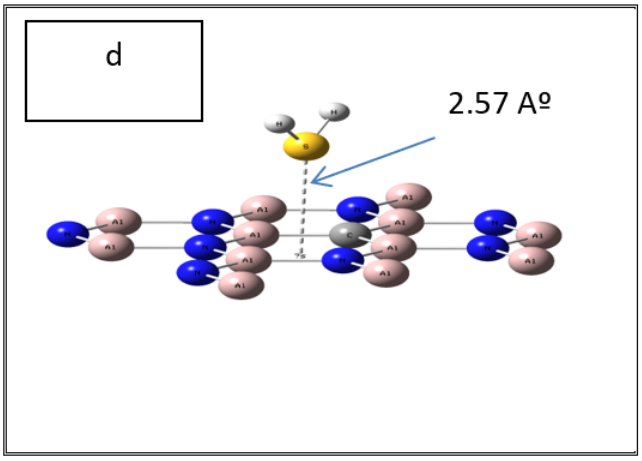


$(AlN)_{20}$–C-$H_2S$ center

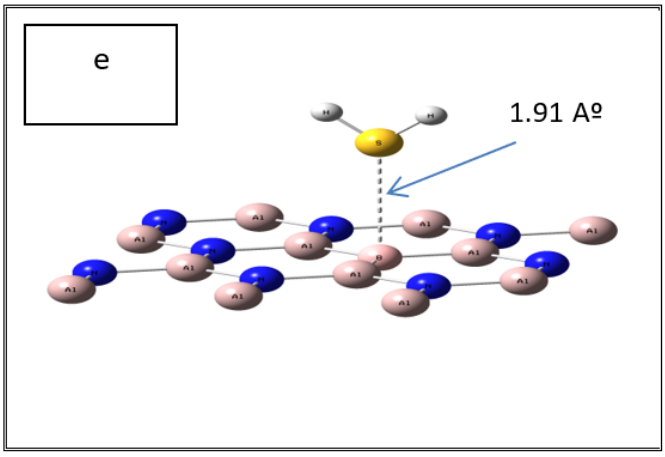


$(AlN)_{20}$–B-$H_2S$

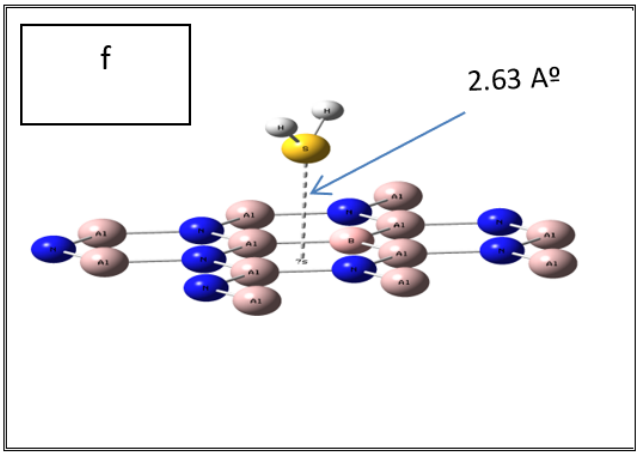


$(AlN)_{20}$–B-$H_2S$ center

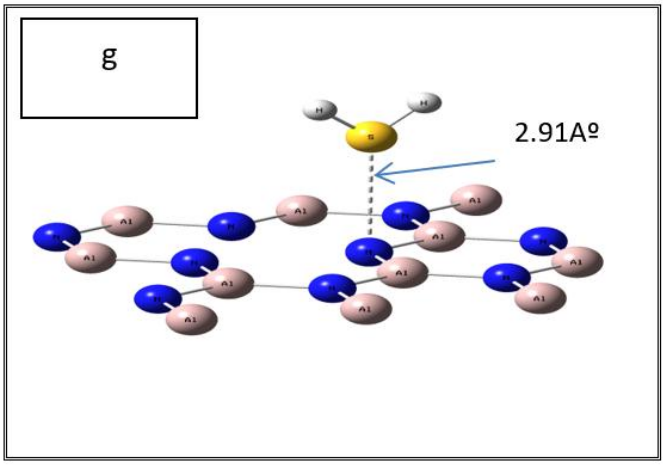


D-P$(AlN)_{20}$–$H_2S$

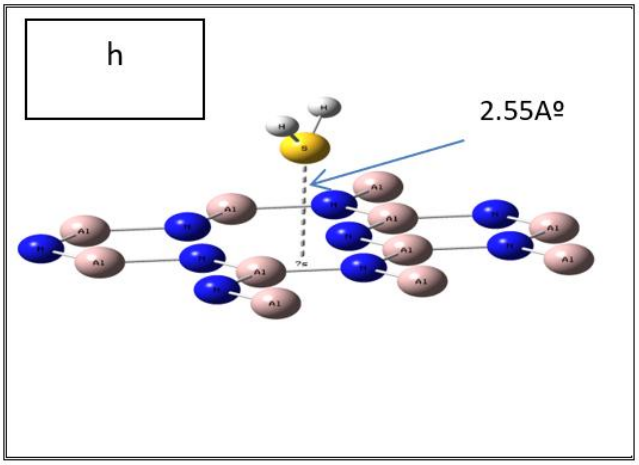


D-P$(AlN)_{20}$-$H_2S$ center

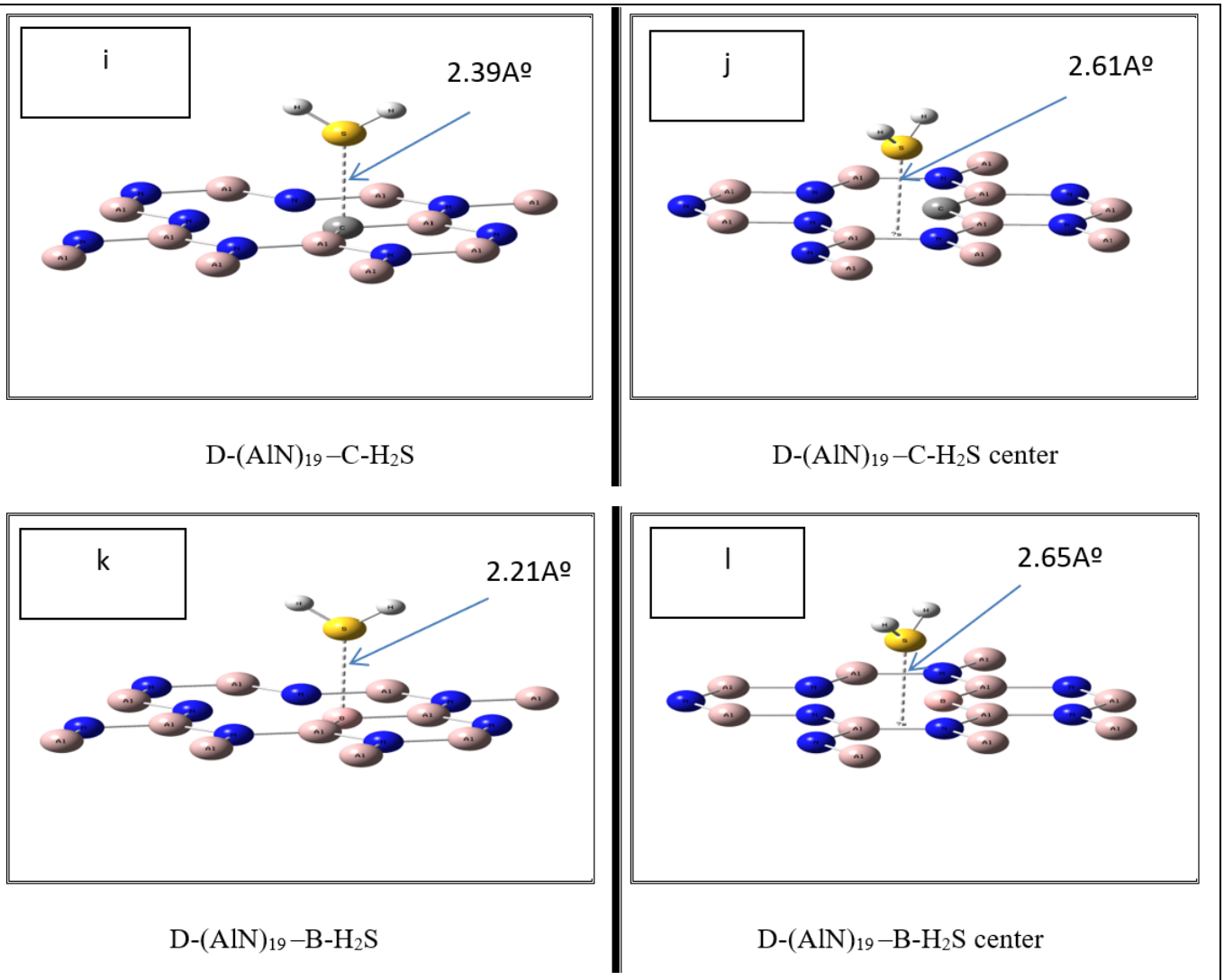


**Figure (1): Initial structures of the studied complexes with $H_2S$ gas.**

With respect to Table (1), it can be noticed that $E_{Tot}$ for adsorption of $H_2S$ on (C, B) atoms-doped $P(AlN)_{20}$ sheet , D-$P(AlN)_{20}$ and D-(C, B)atoms-doped $P(AlN)_{19}$and (adsorption center) are smaller than adsorbed $P(AlN)_{21}$ sheet, this indicates that $E_{Tot}$ increases (in magnitude) with increasing the number of atoms, decreases (in magnitude) with decreasing the number of atoms. And the adsorption energy ($E_{ad}$) of $H_2S$ on the $P(AlN)_{21}$ , (C, B) atoms-doped $(AlN)_{20}$ sheet , D-$P(AlN)_{20}$ and D-(C, B)atoms-doped $P(AlN)_{19}$ sheet are as follow (**-0.468**eV ),( **-0.473** eV ),( **-0.696** eV), (**-0.457** eV), (**-0.478** eV) and (**-0.454** eV) respectively. While ($E_{ad}$) of $H_2S$ on the center ring of the $P(AlN)_{21}$ , (C, B) atoms-doped $(AlN)_{20}$ sheet , D-$P(AlN)_{20}$ and D-(C, B)atoms-doped $(AlN)_{19}$ sheet are (**-0.280** eV ),( **-0.465** eV ),( **-0.646** eV), (**-0.405** eV), (**-0.468** eV) and **-0.282** eV) respectively, $E_{ad}$ of a gas atom are found using equation (3), However, the $E_g$ of $H_2S$ on the $P(AlN)_{21}$ , (C, B) atoms-doped $(AlN)_{20}$ sheet , D-$P(AlN)_{20}$ and D-(C, B) atoms-doped $(AL\text{-}N)_{19}$ sheet are (**2.948** eV ),( **2.231** eV ),( **2.895** eV), (**1.420** eV), (**1.984** eV) and (**2.587** eV) respectively .While ($E_g$) of $H_2S$ on the center ring of the $P(AlN)_{21}$ , (C, B) atoms-doped $P(AlN)_{20}$ sheet , D-$P(AL\text{-}N)_{20}$ and D-(C, B)atoms-doped $P(AlN)_{19}$ sheet are (**2.930** eV), (**2.805** eV),( **2.084** eV), (**0.718** eV), (**1.297** eV), and (**1.929** eV), respectively, $E_g$ of a gas atom are found using equation:

$$Eg = \varepsilon_{LUMO} - \varepsilon_{HOMO} \qquad (5)$$

while the $E_g$ for adsorption of $H_2S$ on D-(C, B)atoms-doped $P(AlN)_{19}$ sheet are smaller than those pristine and no defect molecules, which

indicates that the $E_g$ decreases with the adsorption of $H_2S$ on D-(C, B)atoms-doped $P(AlN)_{19}$. One can observe from the overall results that are displayed in Table (1), The $E_{ad}$ of (B) atoms-doped $P(AlN)_{20}$ sheet (on atom B and center ring) is larger than $E_{ad}$ for another systems because decreasing the number of atoms leads to decrease the area surface on sheets. The $E_{ad}$ of (B) atoms-doped $P(AlN)_{20}$ sheet , (on atom B and center ring) is larger than -0.59 eV, corresponding to strong chemisorption [16]. The $E_{ad}$ for another systems (on atom B and center ring) is smaller than -0.519 eV, corresponding to weak physisorption [17]. The $E_{ad}$ for (B) atoms-doped $P(AlN)_{20}$ sheet (on atom B and center ring) is in agreement with the previous results [18,19]. In general, the $E_{ad}$ of the current results indicates that (B) atoms-doped $P(AlN)_{20}$ sheet is strongly reactive to molecule $H_2S$, the $E_{ad}$ is (-0.696 eV)and (-0.646 eV) $_{\text{center ring}}$, respectively corresponding to a strong chemisorption. Therefore, due to gas slow desorption from (B) atoms-doped $P(AlN)_{20}$, the B-doped $P(AlN)_{20}$ is not suitable . Nevertheless, B-doped $P(AlN)_{20}$ could catalyst or activate this adsorbate due to the strong interaction, suggesting the possibility of B-doped $P(AlN)_{20}$ as a catalyst. For B-doped $P(AlN)_{20}$ and B-doped $P(AlN)_{20})$ $_{\text{center ring}}$, the binding strength of $H_2S$ with B-doped $P(AlN)_{20}$ and( B-doped $P(AlN)_{20}$) center ring are $E_{ad}$ of (-0.696 eV)eV and (-0.646 eV) center ring, respectively, The results of $E_{ad}$ for B-doped $P(AlN)_{20}$ are consistent with those reported in other studies [20]. So the adsorption of $H_2S$ on $P(AlN)_{21}$ , (C) atom-doped $P(AlN)_{20}$ sheet , D-$P(AlN)_{20}$ and D-(C,B) atom-doped $P(AlN)_{19}$ sheet(on atom B and center ring) are weak physisorption, This is because the $E_{ad}$ of this molecules are smaller than -0.518 eV. Thus, $P(AlN)_{21}$ , (C) atom-doped $P(AlN)_{20}$ sheet , D-$P(AlN)_{20}$ and D-(C,B) atom-doped $P(AlN)_{19}$ sheet(on atom B and center ring) can be used to detect $H_2S$ since the adsorption-desorption equilibrium of $H_2S$ on this sheets are easily built.

**Table (1): Structural and electronic properties of adsorption of $H_2S$ molecules on $P(AlN)_{21}$ , (C, B) atoms-doped $P(AlN)_{20}$ , D-$P(AlN)_{20}$ and D-(C, B)atoms-doped $P(AlN)_{19}$ sheets:**

| sutructural | $E_T$ eV | $E_{ads}$ eV | HO eV | LU eV | Eg eV | Ef eV | Q Mulliken |
|---|---|---|---|---|---|---|---|
| $P(AlN)_{21}$-$H_2S$ | -103452.8173 | -0.468012 | -5.512746 | -3.314178 | 2.9485 | -4.4134 | -0.062 |
| $P(AlN)_{21}$-$H_2S$ center | -103452.6295 | -0.280263 | -5.627028 | -2.696511 | 2.9305 | -4.1617 | -0.07 |
| $(AlN)_{20}$-C-$H_2S$ | -102997.33 | -0.473454 | -5.186226 | -2.955006 | 2.2312 | -4.0706 | -0.164 |
| $(AlN)_{20}$-C-$H_2S$ center | -102997.3219 | -0.465291 | -5.463768 | -2.658417 | 2.8053 | -4.0610 | -0.097 |
| $(AlN)_{20}$-B-$H_2S$ | -102635.5187 | -0.696576 | -5.455605 | -2.560461 | 2.8951 | -4.0080 | -0.075 |
| $(AlN)_{20}$-B-$H_2S$ center | -102635.2683 | -0.646244 | -5.444721 | -3.360435 | 2.0842 | -4.4025 | -0.087 |

| D-P(AlN)$_{20}$-H$_2$S | D-P(AlN)$_{20}$-H$_2$S center | D-(AlN)$_{19}$-C-H$_2$S | D-(AlN)$_{19}$-C-H$_2$S center | D-(AlN)$_{19}$-B-H$_2$S | D-(AlN)$_{19}$-B-H$_2$S center |
|---|---|---|---|---|---|
| -96851.86718 | -96851.81548 | -96396.57041 | -96396.55953 | -96038.43511 | -96038.26369 |
| -0.457128 | -0.405429 | -0.478896 | -0.468012 | -0.454407 | -0.282984 |
| -5.591655 | -4.149525 | -5.744031 | -5.403906 | -5.186226 | -4.228434 |
| -4.171293 | -3.431181 | -3.795795 | -4.105989 | -2.598555 | -2.299245 |
| 1.4203 | 0.7183 | 1.9482 | 1.2979 | 2.5876 | 1.9291 |
| -4.8814 | -3.7903 | -4.7699 | -4.7549 | -3.8923 | -3.2638 |
| -0.164 | -0.093 | 0.142 | -0.1 | 0.152 | -0.089 |

upshifts during the interaction of gas with pristine and defective sheets, indicating the electron gain from gas. The charge transfer between gas and P-sheets was obtained from Mulliken population analysis (Table 1).The total Mulliken charge on the molecules, and negative number means charge transfer from sheet to molecule gas.

Figure (2) represents the molecular orbital analysis of the frontier orbitals for studied adsorption molecule on the sheet are obtained at B3LYP/6-31G(d,p) level of theory. In the P(AlN)$_{21}$ sheet lobe. The calculated HOMO, LUMO, energy gap (Eg) values and the corresponding Fermi energies for the pristine, P(AlN)$_{21}$ sheet ,doped pristine, P(AlN)$_{21}$ sheet and defective pristine, P(AlN)$_{21}$ sheets along with gas are summarized in Table (1). The orbital energy shape (Figure 2) shows a considerable change in HOMO and LUMO regions upon adsorption of gas in the pristine, doped and defective P(AlN)$_{21}$ sheets، which illustrates the influence of gas .Both HOMO and LUMO energies of pristine ,doped and defective P(AlN)$_{21}$ sheets are increased upon the adsorption of gas.This indicates the enhancement of electron donating and accepting ability of the P(AlN)$_{21}$ sheet and gas. Furthermore, the gas adsorbed P(AlN)$_{21}$ sheet had large shift in HOMO and LUMO values as illustrated in Table(1) due to the high charge transfer when compared with other gas.Since the increase in energy gap values suggests that the gas are freely entering into the P(AlN)$_{21}$ sheets resulting in the accumulation of charges. Besides from Table (1). the Eg value of the P(AlN)$_{21}$ sheets with gas is greater, (C, B) atoms-doped P(AlN)$_{20}$ sheet , and D-P(AlN)$_{20}$ sheet). Though the adsorption of gas on vacancy defected sheets have a larger than energy gap defects pristine before adsorption gas,. The influence of defects on the shape of pristine and defective sheets before the adsorption of gas in Figure can be seen (2).From figure, D-( B) atom-doped P(AlN)$_{19}$ sheet have minor variations while the other doped and defective have significant variations in the valence band region. Initially, the Fermi level of the pristine sheet is located at(−4.413 eV), (−4.161 eV) $_{\text{center}}$ and the inclusion of defect. leads to the minimize of the valence band, which subsequently shifts the Fermi level to( −3.263 eV). Moreover, the Fermi level of doped and defected sheets, are found to be shifted to −4.70 eV , −4.008 eV −4.881 eV, (−4.769 eV), (−4.892 eV) and (−4.061 eV) $_{\text{center}}$ (−4.402 eV) $_{\text{center}}$ (-3.790eV) $_{\text{center}}$, (-4.754 eV) $_{\text{center}}$,(-3.263 eV) $_{\text{center}}$ ,respectively. Thus, the inclusion of

vacancy defected sheet is responsible for the height reduction of shape lobs in the valence band region. Moreover, the Fermi energy.

| | | |
|---|---|---|
| 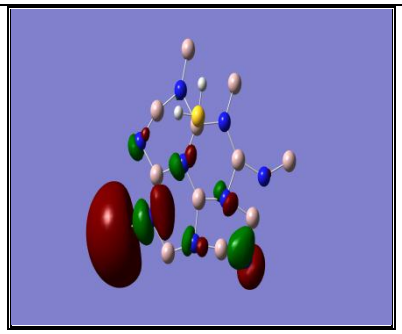 HOMO | $E_g$=2.9305 eV $P(AlN)_{21}$-$H_2S$ center | 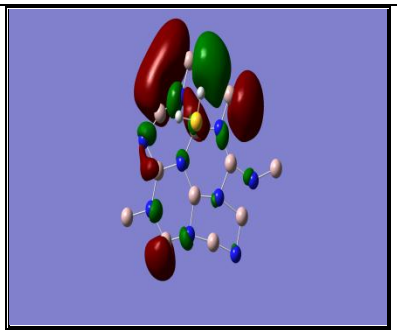 LUMO |
| 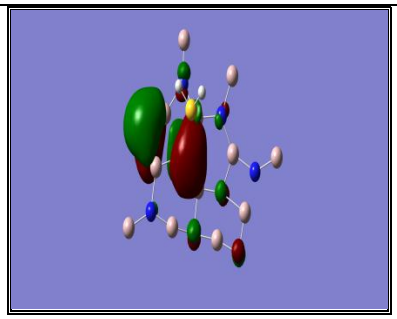 HOMO | $E_g$=2.2312 eV $(AlN)_{20}$-C-$H_2S$ | 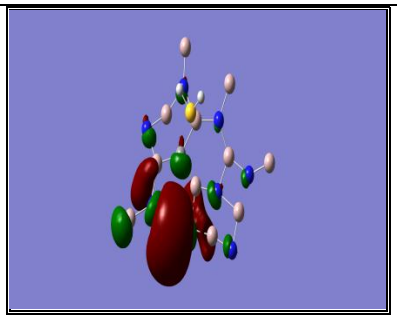 LUMO |
| 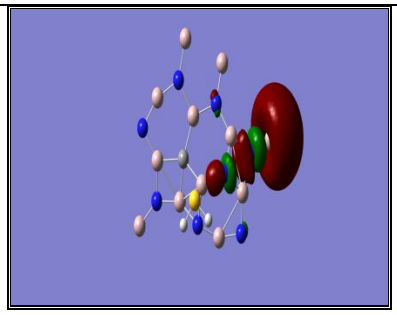 HOMO | $E_g$=2.8053 eV $(AlN)_{20}$-C-$H_2S$ center | 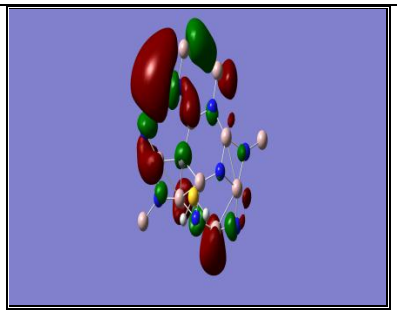 LUMO |
| 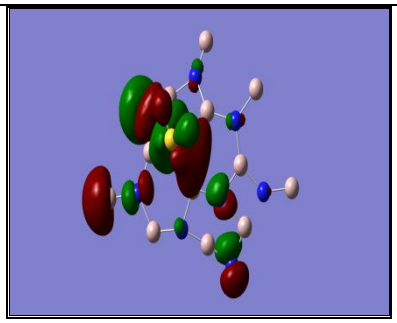 HOMO | $E_g$=2.8951 eV $(AlN)_{20}$-B-$H_2S$ | 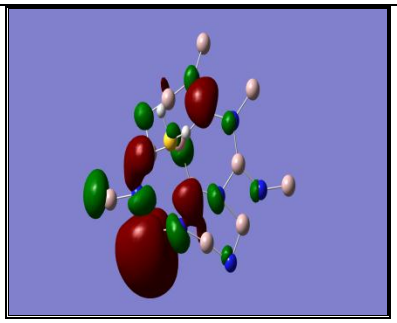 LUMO |
| 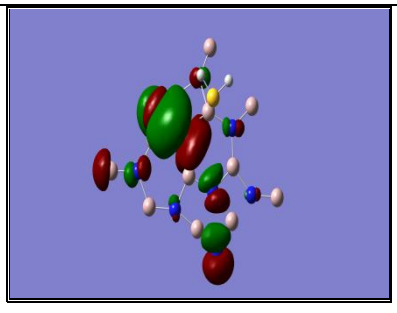 | $E_g$=2.0842 eV $(AlN)_{20}$-B-$H_2S$ center | 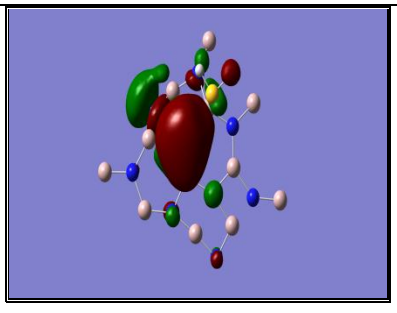 |

| HOMO | | LUMO |
|---|---|---|
| 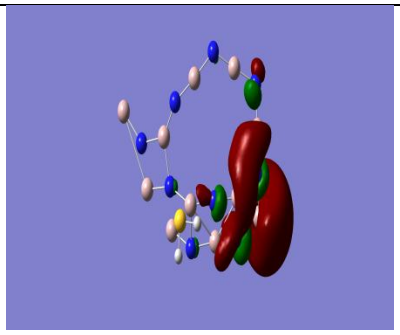 HOMO | $E_g$=1.4203 eV D-P$(AlN)_{20}$-$H_2S$ | 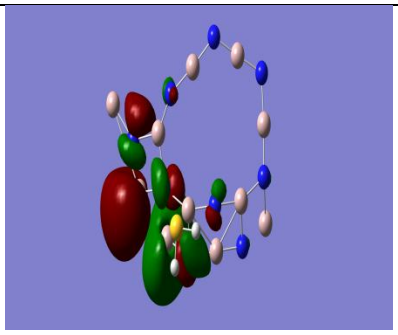 LUMO |
| 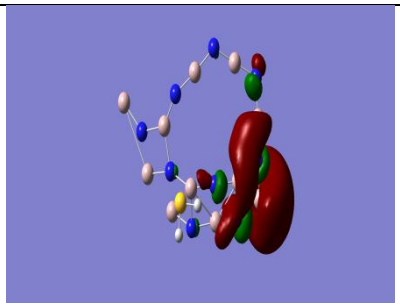 HOMO | Eg=0.7183eV D-P$(AlN)_{20}$-$H_2S$ center | 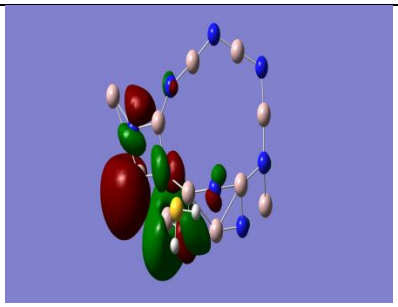 LUMO |
| 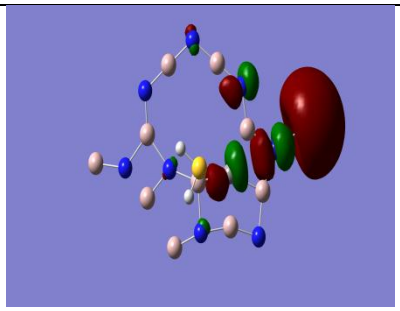 HOMO | Eg=1.9482 eV D-$(AlN)_{19}$-C-$H_2S$ | 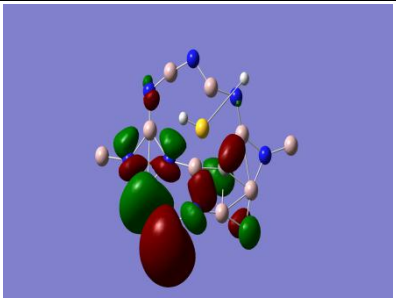 LUMO |
| 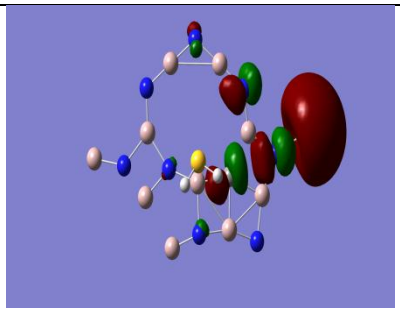 HOMO | Eg=1.2979 eV D-$(AlN)_{19}$-C-$H_2S$ | 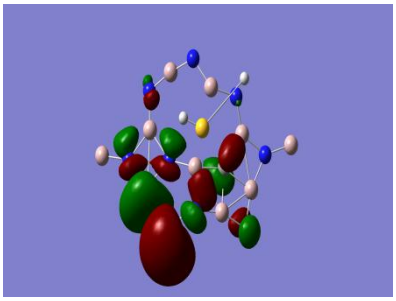 LUMO |
| 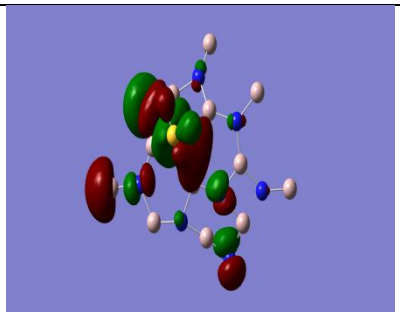 HOMO | Eg=2.5876 eV D-$(AlN)_{19}$-B-$H_2S$ | 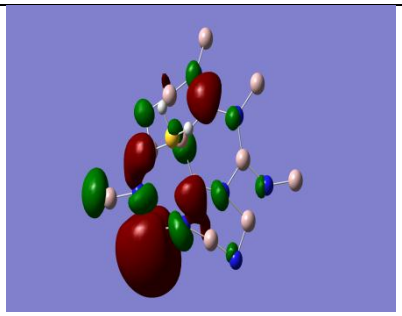 LUMO |

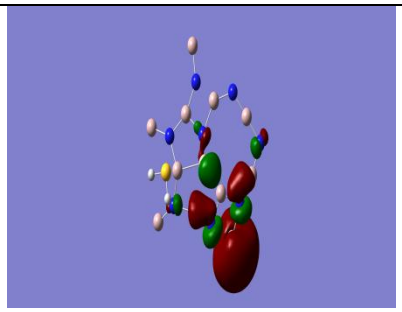

HOMO

Eg=1.9291 eV

D-$(AlN)_{19}$-B-$H_2S$

center

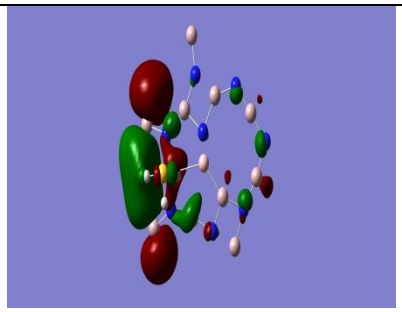

LUMO

**Figure (2): shows the DFT calculation of HOMO and LUMO shapes for studied $H_2S$ adsorption molecules.**

## 4. Conclusion

The conclusions of the present study regarding the adsorption of gases $H_2S$, can be summarized as follows:

1. Good relaxation was obtained for the studied compounds by using the B3LYP-DFT / 6-31G(d,p) basis set. The calculated values of geometrical parameters of the compounds are in a good agreement with other studies.
2. There is no distortion in the planar structure of **P**(AlN) sheet in the case of doping (C,B)-doped **P**(AlN) . The adsorption of gas molecules on $P(AlN)_{21}$ , (C- atoms-doped $P(AlN)_{20}$ sheet , D-$P(AlN)_{20}$ and D-(C, B)atoms-doped $P(AlN)_{19}$ sheet undergoes a weak physisorption interaction, this $E_{ad}$ ranging can be used to detecting gas molecules $H_2S$ .
3. Pristine $P(AlN)_{21}$ , (C- atoms-doped $P(AlN)_{20}$ sheet , D-$P(AlN)_{20}$ and D-(C, B)atoms-doped $P(AL-N)_{19}$ sheet can be used as a good sensor for $H_2S$ and not suitable for usage as a gas sensor for B-doped **P**$(AlN)_{20}$ .
4. The adsorption B-doped **P**$(AlN)_{20}$sheet, on atom and center ring of gas molecule with $H_2S$ undergo in a strong chemisorption interaction with $E_{ad}$ ranging from -0.69 eV to 12.5 eV , so it presumably unsuitable for usage as a gas sensor for these gases, and could catalyse or activate.
5. The values of $E_g$ decrease for adsorbed gases on molecular study
6. Pristine **P**(AlN) sheet, doped and defect are more sensitive to the $H_2S$ based toxic gases.

The electronic properties of **P**(AlN) can be modified by doped **P**(AlN) and defective **P**(AlN) sheets.

## 5. REFERENCES

[1] Aghaei SM, Monshi MM, Torres I, Calizo I. Adsorption and Dissociation of Toxic Gas Molecules on Graphene-like BC3: A Search for Highly Sensitive Molecular Sensors and Catalysts. arXiv preprint arXiv:1706.00774. 2017 Jun 2.

[2] Nasehnia F, Seifi M. Adsorption of molecular oxygen on VIIIB transition metal-doped graphene: A DFT study. Modern Physics Letters B. 2014 Dec 10;28(30):1450237.

[3] Ma L, Zhang JM, Xu KW, Ji V. A first-principles study on gas sensing properties of graphene and Pd-doped graphene. Applied Surface Science. 2015 Jul 15;343:121-7.

[4] Giovannetti GA, Khomyakov PA, Brocks G, Karpan VV, Van den Brink J, Kelly PJ. Doping graphene with

metal contacts. Physical review letters. 2008 Jul 10;101(2):026803.

[5] Mohmmed HS, Abo Nasriya AH. Study electronic properties of adsorption of CO and H2S gas molecules on the surface of fullerene and heterofullerene as a gas sensor for environmental protection of organic and pharmaceutical material. Journal of Global pharma Technology. 2017;10(9):11-8.

[6] Latif, U. and Dickert, F.L., 2015. Graphene hybrid materials in gas sensing applications. Sensors, 15(12), pp.30504-30524.

[7] Zou Y, Li F, Zhu ZH, Zhao MW, Xu XG, Su XY. An ab initio study on gas sensing properties of graphene and Si-doped graphene. The European Physical Journal B. 2011 Jun 1;81(4):475-9.

[8] Nasria AH. Electronic properties of phosphorene nanoribbons doped with boron, aluminum and carbon. J. Chem. Pharm. Sci. 2017;10(2):935-9.

[9] Abbas OA, Omran AH, Rahim AH. The effect of different wavelengths on porous silicon formation process. Univ Babylon J. 2008;1(1):75.

[10] Abbas OA, Noman KA, Rahim AH. Effect of Different Etching Parameters on Resistivity of Silicon Nano-Material. Journal of Kufa-physics. 2009;1(2 English):100-7.

[11] Raheem AH, Al-Shejyri KJ, Al-bermany ED. Density Functional Theory Calculations For MethylBenzene Molecules group.

[12] Al-Sukkry LM, Abo Nasriya AH. DFT Investigation of CH2O adsorption on pristine and doped Fullerene C32. ISJ Theoretical & Applied Science, 09 (77). 2019:337-40.

[13] Henry DJ, Parkinson CJ, Mayer PM, Radom L. Bond dissociation energies and radical stabilization energies associated with substituted methyl radicals. The Journal of Physical Chemistry A. 2001 Jul 12;105(27):6750-6.

[14] Frisch MJ, Trucks GW, Schlegel HB, Scuseria GE, Robb MA, Cheeseman JR, Scalmani G, Barone V, Mennucci B, Petersson GA, Nakatsuji H. M. J. Frisch, G. W. Trucks, H. B. Schlegel, G. E. Scuseria, M. A. Robb, J. R. Cheeseman, G. Scalmani, V. Barone, B. Mennucci, G. A. Petersson, H. Nakatsuji, M. Caricato, X. Li, H. P. Hratchian, A. F. Izmaylov, J. Bloino, G. Zheng, J. L. Sonnenberg, M. Hada, M. Ehara, K. Toyota, R. Fukuda, J. Hasegawa, M. Ishida, T. Nakajima, Y. Honda, O. Kitao, H. Nakai, T. Vreven, J. A. Montgomery, Jr., J. E. Peralta, F. Ogliaro, M. Bearpark, J. J. Heyd, E. Brothers, K. N. Kudin, V. N. Staroverov, R. Kobayashi, J. Normand, K. Raghavachari, A. Rendell, J. C. Burant, S. S. Iyengar, J. Tomasi, M. Cossi, N. Rega, J. M. Millam, M. Klene, J. E. Knox, J. B. Cross, V. Bakken, C. Adamo, J. Jaramillo, R. Gomperts, R. E. Stratmann, O. Yazyev, A. J. Austin, R. Cammi, C. Pomelli, J. W. Ochterski, R. L. Martin, K. Morokuma, V. G. Zakrzewski, G. A. Voth, P. Salvador, J. J. Dannenberg, S. Dapprich, A. D. Daniels, O. Farkas, J. B. Foresman, J. V. Ortiz, J. Cioslowski, and D. J. Fox, Gaussian 09, revision A. 02, Gaussian, Inc., Wallingford, CT, 2009 Search PubMed;(b) C. Lee, W. Yang and RG Parr. Phys. Rev. B: Condens. Matter Mater. Phys. 1988;37:785.

[15] Ouyang T, Qian Z, Ahuja R, Liu X. First-principles investigation of CO adsorption on pristine, C-doped and N-vacancy defected hexagonal AlN nanosheets. Applied Surface Science. 2018 May 1;439:196-201.

[16] Leeuwen RV, Baerends EJ. An analysis of nonlocal density functionals in chemical bonding. International journal of quantum chemistry. 1994 Nov 5;52(4):711-30.

[17] Politzer P, Seminario JM, editors. Modern density functional theory: a tool for chemistry. Elsevier; 1995 Jan 27.

[18] Jensen F. Introduction to computational chemistry. John wiley & sons; 2017 Feb 6.

[19] Stephens PJ, Devlin FJ, Chabalowski CF, Frisch MJ. Ab initio calculation of vibrational absorption and circular dichroism spectra using density functional force fields. The Journal of physical chemistry. 1994 Nov;98(45):11623-7.

[20] . Baei MT, Peyghan AA, Bagheri Z. Fluorination of the exterior surface of AlN nanotube: a DFT study. Superlattices and Microstructures. 2013 Jan 1;53:9-15.